International Journal of Mass Spectrometry and Ion Processes, 107 (1991) 453–474
Elsevier Science Publishers B.V., Amsterdam

INFLUENCE OF ELECTRONIC EXCITATION IN THE CHARGE REVERSAL OF HALOGENATED CATIONS

BERNARD LEYH and HUGUETTE WANKENNE

Département de Chimie – Bâtiment B6, Université de Liège, 4000 Sart-Tilman Liège I (Belgium)

(First received 28 December 1990; in final form 11 March 1991)

ABSTRACT

Charge reversal of high kinetic energy (8 keV) cations during collisions with atomic target gases (G = Xe, Kr, Ne) has been studied for CCl_n^+ ($n = 1$ or 2) ions resulting from dissociative electroionization of CCl_4.

The influence of electronic excitation of the incident cation CCl_n^+ and of the nature of the target gas G on the anion yield have been examined. In our experiments, the two-collision process $CCl_n^+ \xrightarrow[\text{step a}]{G} CCl_n + G^+ \xrightarrow[\text{step b}]{G} CCl_n^- + 2G^+$ is predominant. By comparing the anion and cation yields as a function of the kinetic energy of the ionizing electrons, we found evidence, with some target gases, of the existence of long-lived excited states of CCl^+ and CCl_2^+, which lead to an increase in the anion yield in comparison with charge reversal of the corresponding ground state ions. For CCl^+, we deduce an excitation energy of 4 ± 1 eV with a lifetime longer than 6.2 μs. These results are compatible with the $a^3\Pi$ long-lived state of CCl^+ previously detected by optical spectroscopy and by charge-stripping experiments. Our experimental data on charge reversal and metastable dissociation of CCl_2^+ reveal the existence of a long-lived state (lifetime > 8.2 μs) of CCl_2^+ lying at 4.3 ± 1 eV above the ground state. Semi-empirical MNDO calculations show that the energy of the first quartet state, $\tilde{a}^4A_2$, is compatible with the observed excitation energy. The spin–orbit coupling-induced transition from the $\tilde{a}^4A_2$ state to the $\tilde{B}^2A_2$ state is suggested to play an important role in the metastable dissociation $CCl_2^{+*} \rightarrow CCl^+ + Cl$.

The origin of the increase in the anion yield when long-lived excited states of CCl^+ and CCl_2^+ are charge-reversed is discussed. Step a is suggested to be responsible for this yield enhancement which is observed when an appropriate target gas makes this step quasi-resonant.

INTRODUCTION

Tandem mass spectrometry has proved to be a powerful technique for the elucidation of the structure of ions and for the study of their reactivity [1,2]. For about two decades, MS–MS has been successfully applied, as an analytical tool, for structure elucidation and mixture analysis in various fields, such as biomedical research, forensic applications, polymers, etc. [2]. In the great majority of these studies, the energy necessary to dissociate the primary ions is provided by collisional activation (CAD) [1–6]. Other methods of ion

activation based on collisional processes have also been developed; in such methods, the charge state of the ion is modified upon neutralization [7–10], charge stripping [11–15] or charge reversal [16–22]. In some instances, these new activation techniques can lead to fragmentation patterns which are more structurally diagnostic than the usual CAD spectra. However, such collisional processes can lead to the formation of neutral or ionic species of unconventional structures which would be very difficult to obtain by other techniques [10].

Despite the numerous applications which we have mentioned, the basic processes which govern the collisional processes involved have been rarely studied and are thus poorly understood even for usual CAD. Our understanding is particularly poor as far as polyatomic projectiles and/or targets is concerned.

In this paper, we analyse the influence of electronic excitation in the starting cation in charge reversal processes such as

$$M^+ + G \rightarrow M^- + G^{2+} \quad (1)$$

$$M^+ + 2G \rightarrow M^- + 2G^+ \quad (2)$$

where M^+ is the fast (kinetic energy = 8000 eV) projectile and G is the target gas. The relative yield of process 1 vs. process 2 depends on the target gas pressure. The starting cations which have been chosen are CCl^+ and CCl_2^+ resulting from dissociative electroionization of CCl_4. The target gases used are Xe, Kr and Ne.

I. EXPERIMENTAL

A. Apparatus

All the experiments described in this paper have been carried out using a double-focussing AEI-MS9 mass spectrometer. The positive ions are produced by electron impact using a conventional electron ionization source. The charge reversal processes take place in a differentially pumped floatable collision cell which has been installed in the second field-free region, i.e. between the electrostatic analyser and the magnet. The configuration is therefore the same as that of the MS9 instrument recently modified by Harris and Cooper [23] for double charge transfer (charge reversal) experiments. In contrast to these authors, we record the charge reversal spectra by scanning the magnet after reversal of its polarity. Because of the forward geometry of the MS9, the fragment ions resulting from the dissociation of the negative ions produced by charge reversal appear at apparent masses $m^* = m_2^2/m_1$.

Experiments have also been performed by admitting gas into the first field-free region. Owing to the absence of a collision cell and of differential pumping in this field-free region, the experimental conditions are, however,

ill-defined. Charge reversal of the parent ions is in this case studied by inverting the polarity of both the electrostatic analyser and the magnet and by scanning the magnet. The fragmentation processes of the charge reversed ions are studied by scanning the source accelerating voltage (V scan).

The experimental conditions are as follows: accelerating voltage, 8000 eV; emission current, 100 μA; ion source pressure of CCl_4, $1 - 8 \times 10^{-6}$ Torr; target gas pressure (measured about 20 cm from the cell), typically 2×10^{-5} Torr corresponding to an attenuation of the main beam of 40–60%. CCl_4 is provided by Merck with a graded purity > 99.8% and is used without further purification. The target gases Xe, Ne and Kr, provided by L'air Liquide (purity = 99.99%), are also used without further purification.

The target gas pressure used ensures that double-collision reactions (eqn. 2) dominate (see complete discussion in Sections II.A and III.A). There was therefore no real need to resolve the single (eqn. 1) and double (eqn. 2) collision signals.

The ion yield curves as a function of the kinetic energy, E_k, of the ionizing electrons were determined by tuning the instrument to transmit the ion of interest and by scanning E_k; this method consists therefore of recording peak height variations. A counting technique was used to get the best possible accuracy and sensitivity. The appearance energies of the ions were determined by the vanishing current method [24]; a critical analysis of the different techniques used to determine appearance energies led Beynon et al. [25] to the conclusion that the vanishing current method is the only one which can be used to obtain accurate values. The electron energy scale was calibrated using Xe (ionization energy = 12.13 eV), Kr (14.00 eV), and He (24.59 eV) as references.

B. Data handling

In order to analyse the possible influence of electronic excitation in the starting cation on the cross-section for charge reversal, we have compared the ion yield curves as a function of the kinetic energy of the ionizing electrons, I vs. E_k, for the positive ions and for the negative ions resulting from charge reversal.

The ion yield curve, I^+, for a positive ion M^+ at low electron energy (i.e. not too far from the first ionization threshold) consists ideally of a series of straight lines corresponding to the different vibronic states of the ion [26]. Let us now consider the charge reversal of M^+ in a given excited electronic state to give M^- and analyse the yield I^- of M^- ions as a function of E_k. Two typical situations can be encountered. If the excited electronic state has a lifetime with respect to fluorescence or internal conversion shorter than the travel time between the ion source and the collision cell (typically 5–10 μs),

every cation before charge reversal will be in its ground electronic state. In such a situation, $I^-(E_k) = PI^+(E_k)$, where P is the probability of charge reversal which depends on the cross-section, on the target gas pressure and on the collision cell geometry:

$$P = 1 - \exp(-n\sigma L) \tag{3}$$

A second situation occurs if the first excited state has such a lifetime that it survives up to the collision event. In this case, two charge reversal probabilities must be taken into account, P_0 and P_1, for the ground and excited states respectively. For the sake of simplicity, we consider that M^- is stable only in its ground electronic state. In such a case, still considering the threshold laws, we can write:

$$AE_0 < E_k < AE_1: \quad I^-(E_k) = P_0 I^+(E_k) \tag{4a}$$

$$AE_1 < E_k < AE_2: \quad I^-(E_k) = P_0 f_0(E_k) I^+(E_k) + P_1 f_1(E_k) I^+(E_k) \tag{4b}$$

where AE_i is the appearance energy of M^+ in its state i; $f_i(E_k)$ is the probability that M^+ is in the state i as a function of E_k: $f_0 + f_1 = 1$. Generally, $f_0 \gg f_1$.

In conclusion, any change in the shape of $I^-(E_k)$ compared with that of $I^+(E_k)$ results from the involvement of an excited state of M^+ whose lifetime is longer than the flight time between the source and the collision cell. To make the data easier to visualize, we have plotted the ratio of I^-/I^+ for a given ion. Dividing eqn. 4 by I^+ gives:

$$AE_0 < E_k < AE_1: \quad I^-/I^+(E_k) = P_0 \tag{5a}$$

$$AE_1 < E_k < AE_2: \quad I^-/I^+(E_k) = P_0 f_0(E_k) + P_1 f_1(E_k) \tag{5b}$$

This results in a change in the first derivative of I^-/I^+ (from zero to a positive or negative value) at $E_k = AE_1$. Owing to the usually small f_1 values, a measurable effect will only be obtained if the excited state and the ground state have very different cross-sections for charge reversal.

The data of Fig. 1 illustrate the case where no long-lived excited state is present. The I^-/I^+ ratio has been measured for the $OH^+ \rightarrow OH^-$ charge reversal. The OH^+ ions result from the dissociative electroionization of water and Kr is used as a target gas at a pressure corresponding to a 60% transmittance of the positive ion beam. It is known from high resolution kinetic energy spectroscopy that more than 99.8% of such OH^+ ions are in their ground electronic state when they leave the ion source [27]. We observe indeed that the I^-/I^+ ratio remains constant within experimental error ($I^-/I^+ = 0.95 \pm 0.12$) over all the energy region investigated (up to 7 eV above the threshold). The $CCl^+ \rightarrow CCl^-$ charge reversal, which will be discussed in detail in Section II, illustrates the situation where a long-lived excited state plays a role in the charge permutation (Fig. 3, to be discussed later).

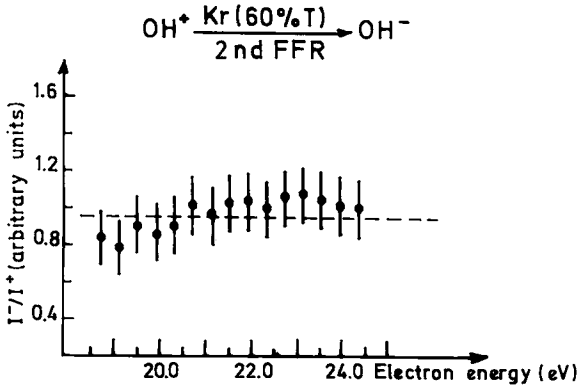

Fig. 1. Ratio of the anionic current to the cationic current, I^-/I^+, as a function of the kinetic energy of the ionizing electrons. The OH^+ ions result from the dissociative electroionization of H_2O. Their kinetic energy is equal to 8000 eV.

Great care has to be taken when comparing the I^- and I^+ curves whose shapes can depend strongly on the experimental conditions (especially the ion source pressure). Only I^- and I^+ curves obtained under strictly identical conditions have been compared. As the pressure within the ionization chamber cannot be measured directly, it has been estimated in the following way [24]: the total ion current of various rare gases and of nitrogen was collected at the ion repeller on which a weak negative potential was applied; the measurement of this ionic current, together with the knowledge of the electron emission current and the ionization cross-section allows us to determine the number of particles per unit of volume (see eqn. 3) and thus to determine the pressure within the ionization chamber for a given reading at the ion gauge. Even with the highest pressure used (8×10^{-6} Torr at the ion gauge $= 1.5 \times 10^{-4}$ Torr in the ionization chamber), the mean free path is still larger than 70 cm. Furthermore, the ion signal has been checked for linearity in all the source pressure domain used, for both the positive and negative ions. The I^+ curves have been recorded without gas in the collision cell to avoid any perturbation by the variety of collisional processes which could take place if a target gas was present. We have, however, checked, in the CCl^+ case, that the influence of introducing a target gas into the collision cell on the I^+ curves was negligible.

II. THE $CCl^+ \rightarrow CCl^-$ CHARGE REVERSAL

A. Experimental results

Figure 2 shows the ion yield curves $I^+(E_k)$ and $I^-(E_k)$ for CCl^+ from CCl_4. The increase of the positive ion signal at the threshold is very slow (Fig. 2a):

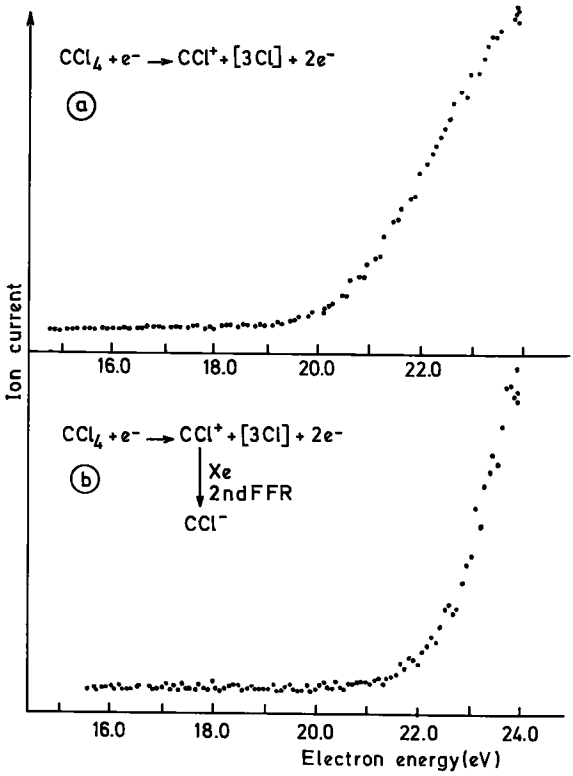

Fig. 2. Cationic (a) and anionic (b) currents as a function of the kinetic energy of the ionizing electrons. The CCl^+ ions (kinetic energy = 8000 eV) result from dissociative electroionization of CCl_4. The negative ions are obtained by charge reversal of CCl^+ upon collision with Xe atoms. The transmittance of the positive ion beam is equal to 40%.

the AE value which can be deduced by the vanishing current method is 18.0 ± 0.5 eV, which is significantly lower than the 19.35 eV usually reported [28]. The comparison with the thermodynamical threshold for the process

$$CCl_4 \rightarrow CCl^+ + \text{neutrals} + e^-$$

requires the knowledge of $\Delta H_f^\circ(CCl^+)$. Tornow et al. [29] report a value of $1264 \pm 14\,kJ\,mol^{-1}$ whereas Lias et al. [30] report $1243\,kJ\,mol^{-1}$. According to Tornow et al. [29], a ΔH_r° of $1725\,kJ\,mol^{-1}$ (17.89 eV) can be calculated for the reaction

$$CCl_4 \rightarrow CCl^+ + 3Cl + e^-$$

This value compares well with the AE deduced from Fig. 2a. The lowest energy process

$$CCl_4 \rightarrow CCl^+ + Cl_2 + Cl + e^-$$

requires 2.5 eV less energy and its probability is too low to be observed in our experiments.

The data of Fig. 2b show a much poorer signal-to-noise ratio owing to the low cross-section of the $CCl^+ \rightarrow CCl^-$ process. The variation of this cross-section with the target pressure (Xe in this case) shows that both one- and two-collision processes are present. At our working pressure (see Section I.A.), which corresponds to an attenuation of the main beam of 60%, the probability of the two-collision process is 5.7 times larger than that of the one-collision process. The average number of collisions per affected CCl^+ ion is thus equal to 1.85, in good agreement with the value of 1.75 which can be obtained from the work of Todd and McLafferty [6] for a beam attenuation of 60%. By comparing Figs. 2a and 2b, it can already be seen that the anion signal starts to increase much later than the positive ion signal. This is even clearer in Fig. 3 where the I^-/I^+ ratio, discussed in Section I.B., is displayed. In other words, the cross-section for charge reversal of CCl^+ increases when its internal energy increases. It must be mentioned at this point that I^-/I^+ data at near-threshold E_k values are obtained with a very poor precision because one has to divide by very small numbers: these data are not displayed in Fig. 3.

Other experiments have been performed to obtain complementary information. We have considered the influence of the nature of the target gas. The cross-sections for charge reversal of CCl^+, created by electroionization ($E_k = 40$ eV) of CCl_4, with the target gases Xe, Kr and Ne, are in the ratio 1.0 : 0.33 : 0.20. We have measured the I^-/I^+ ratio for charge permutation with Kr (Fig. 4). In this case, no change is observed at $E_k = 22$ eV: charge reversal with Kr is not favoured by cation excitation. In fact, it is most

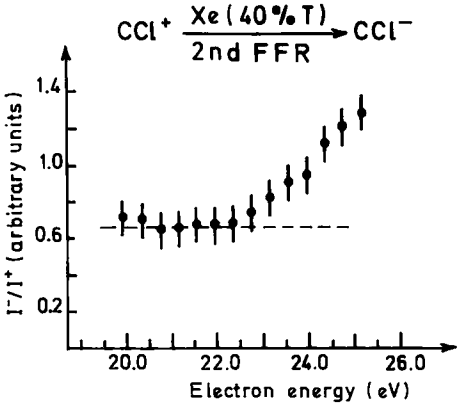

Fig. 3. Ratio of the anionic and cationic currents, I^-/I^+, for charge reversal of CCl^+ upon collision with Xe atoms (transmittance of the main beam = 40%).

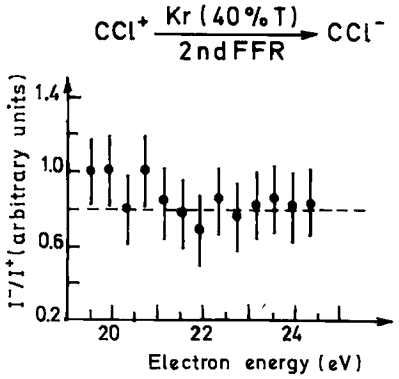

Fig. 4. Ratio of the anionic and cationic currents, I^-/I^+, for charge reversal of CCl^+ upon collision with Kr atoms (transmittance of the main beam = 40%).

probably the first step of the charge inversion process which is not favoured, as discussed at the end of Section II.B.

In Fig. 5, we give the I^-/I^+ ratio for charge reversal of CCl^+ induced by admitting Xe gas in the first field-free region. These data clearly confirm those of Fig. 3.

The dissociative charge reversal of CCl^+ leading to the Cl^- fragment ion has also been investigated by the V scan under the same conditions as in Fig. 5. The corresponding I^-/I^+ ratio is displayed in Fig. 6.

B. Discussion

Let us first discuss the increase in the I^-/I^+ ratio observed at $E_k = 22\,eV$ when Xe is the target gas (Fig. 3): this corresponds to an excitation energy of

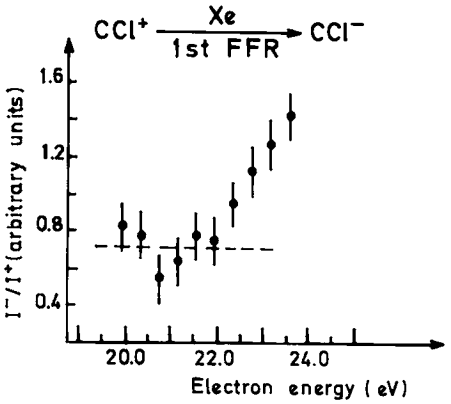

Fig. 5. Ratio of the anionic and cationic currents, I^-/I^+, for charge reversal of CCl^+ upon collision with Xe atoms in the first field-free region.

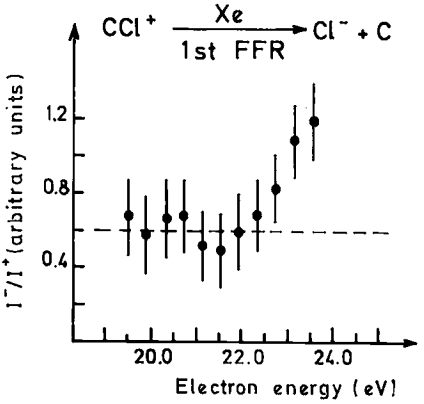

Fig. 6. Ratio of the anionic and cationic currents, I^-/I^+, for dissociative charge reversal of CCl^+ leading to the Cl^- + C fragments. Charge reversal occurs upon collision with Xe atoms in the first field-free region.

(22–18) eV = 4 ± 1 eV. Two possible excited states of CCl^+ can be considered: $A^1\Pi$ and $a^3\Pi$. The singlet state has been observed by Van Sprang et al. [31] in emission cross-section measurements following electron impact at a wavelength of 236.7 nm (5.24 eV). Furthermore, they deduced a radiative lifetime for this state of 3.9 μs, which is shorter than the time needed by CCl^+ to reach the collision cell of our mass spectrometer (6.2 μs), under the experimental conditions described in Section I.A. However, Tsuji et al. [32] observed a state located at longer wavelength (392.4 nm or 3.16 eV) and their assignment to the $a^3\Pi$ state is confirmed by ab initio calculations; this excitation energy is compatible with the above-mentioned value deduced from our charge reversal experiments.

A related, very elegant piece of work by Langford et al. [33] is also in agreement with our data. They studied the charge stripping of various halogenated ions by high-resolution kinetic energy spectroscopy. For CCl^+ from CCl_4, they observed an excited state whose energy is equal to 3 ± 1 eV above the ground state. They assigned it to CCl^+ $a^3\Pi$, according to the work of Tsuji et al. [32], and deduced a lifetime which is in excess of 7.8 μs. Furthermore, when they decreased the energy of the ionizing electrons, they observed that the signal associated with this state vanished at around 22 eV, i.e. exactly the value deduced from our experiments (Fig. 3). Even more closely related to our problem is the work of Griffiths et al. [34] who performed the same kind of kinetic energy spectroscopy on the charge reversal of CF^+ and CCl^+ resulting from dissociative electroionization of $CFCl_3$ and $CF_2ClCFCl_2$. They detected by this method a long-lived excited state for both ions, the excitation energy being equal to 3.3 eV in the CCl^+ case. Dissociative ionization of $CFCl_3$ was shown to produce the largest amount of excited CCl^+.

These various experiments, performed using very different techniques, allow confirmation of both the presence of a triplet excited state of CCl^+ at an energy of 3.2 eV (spectroscopic value) whose lifetime is longer than 8 μs, and its involvement in charge reversal processes (ref. 34 and this paper) as well as in charge stripping [33].

The enhancement of the CCl^- yield upon electronic excitation of CCl^+ to the $a^3\Pi$ state can result from several mechanisms. A first possibility is that the cross-section for charge reversal upon collision with Xe atoms is larger for the a than for the X state. A second possibility is that charge reversal of CCl^+ $X^1\Sigma^+$ could lead to excited CCl^- which would readily dissociate into C + Cl^- or C^- + Cl. Figure 6 shows an increase in the Cl^- yield at the same E_k value (22 eV) for dissociative charge reversal of CCl^+, and the measured kinetic energy release during Cl^- formation is equal to 0.43 eV. Four mechanisms could be responsible for the Cl^- formation:

$$CCl^+ \xrightarrow{Xe} CCl^{-}* \longrightarrow Cl^- + C \qquad (a)$$

$$CCl^{+}* \longrightarrow Cl^+ + C \xrightarrow{Xe} Cl^- + C \qquad (b)$$

$$CCl^+ \xrightarrow{Xe} Cl^+ + C \xrightarrow{Xe} Cl^- + C \qquad (c)$$

$$CCl^+ \xrightarrow{Xe} CCl* \longrightarrow Cl + C \xrightarrow{Xe} Cl^- + C \qquad (d)$$

Process (b) can be immediately eliminated because it requires at least 23.92 eV [30], the lowest calculated energy for Cl^+ appearance. Moreover, the kinetic energy released during this process should be at least equal to 0.62 eV, which is the value measured for the metastable dissociation of CCl^+. However, in process (c), the collisionally activated dissociation of CCl^+ could appear at lower energy; it is, however, unlikely that less kinetic energy be released upon CAD than in the metastable fragmentation. To investigate the possibility of process (d), useful information would be obtained from neutralization–reionization mass spectrometry experiments. Even though we cannot ignore the fact that part of the Cl^- observed could result from process (d), it seems that process (a) is most probably involved in the Cl^- yield observed at E_k = 22 eV. From the observed increase in Fig. 6 at this energy, we can conclude that the CCl^+ $a^3\Pi$ state plays an important role in the charge reversal of CCl^+ as well as in the associated dissociative process when an Xe target is used. As will be discussed soon, charge reversal occurs within the collision complex $[CCl\cdots Xe]^+$. In the C_s point group, many non-adiabatic interactions will certainly take place; spin-orbit interactions are also expected with a heavy target like Xe. In practice there will therefore be neither spin nor symmetry restrictions for charge reversal from the ground and the first triplet state of CCl^+ and for both the one- and two-step processes.

The fact that electronic excitation does not affect the charge reversal cross-section of CCl^+ when Kr is used as the target gas (Fig. 4) requires some discussion. As we have already mentioned, at our target gas pressure, the two-collision processes are the most probable. The first step of such a process is the neutralization of the projectile and the ionization of the target. It can be observed that neutralization of CCl^+ $a^3\Pi$ has an exothermicity of 8.9 [30] + 3.2 [32] = 12.1 eV and is therefore resonant with the ionization of Xe, which requires 12.1 eV. This could at first sight explain the higher probability of this process. Ionization of Kr, on the other hand, requires 14.0 eV: the resonance condition is far from being realized. However, as Lorquet et al. [35] recently showed, what really matters is the gap between the potential energy surfaces in the region where charge transfer occurs, i.e. within the collision pair $[Xe \cdots CCl^+]$, rather than the asymptotic gap at infinite distance between the collision partners. Three potential energy hypersurfaces (HS) at least have to be considered. They lead to the following asymptotes, ordered as a function of increasing energy: $CCl^+(X^1\Sigma) + Xe(^1S_0)$ (HS1), $CCl^+(a^3\Pi) + Xe(^1S_0)$ (HS2), $CCl(X^2\Pi) + Xe^+(^2P)$ (HS3). Non-adiabatic interactions between these hypersurfaces will bring about the transitions which are responsible for the charge exchange process. The non-adiabatic interactions between HS2 and HS3 will certainly occur at much larger $CCl \cdots Xe$ distances than between HS1 and HS3, as HS2 and HS3 are asymptotically quasi-degenerate. It can be expected that charge transfer at a large distance between the collision partners will be favoured by using a highly polarizable target like Xe. If Kr is used, asymptotic degeneracy between HS1, HS2 and HS3 will no longer exist. Charge exchange will probably occur at shorter $Kr \cdots CCl$ distances. Our experimental data show that both transitions leading to charge exchange are in this case almost equally probable.

III. THE $CCl_2^+ \rightarrow CCl_2^-$ CHARGE REVERSAL

A. Experimental results

Figure 7 shows the ion yield curves $I^+(E_k)$ and $I^-(E_k)$ for CCl_2^+ from CCl_4. The data of Fig. 7b are obtained with Xe as the target gas. From Fig. 7a, an appearance potential for CCl_2^+ of 15.3 eV is obtained. At very high sensitivity, a tiny signal is observed below this limit and vanishes below about 14 eV. The 15.3 eV threshold can be correlated to the

$$CCl_4 \rightarrow CCl_2^+ + 2Cl + e^-$$

process. The thermodynamical threshold for this reaction is equal to 15.58 eV according to Lias et al. [30] and to 15.00 eV according to Rademann et al. [36].

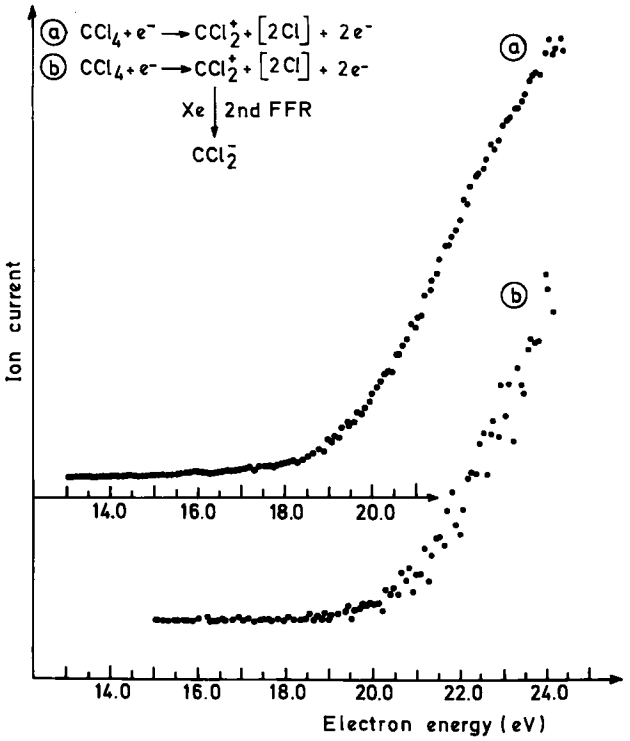

Fig. 7. Cationic (a) and anionic (b) currents as a function of the kinetic energy of the ionizing electrons. The CCl_2^+ ions (kinetic energy = 8000 eV) result from dissociative ionization of CCl_4. The negative ions are obtained by charge reversal of CCl_2^+ upon collision with Xe atoms. The transmittance of the positive ion beam is equal to 40%.

The lowest threshold corresponds most probably to the following process:

$$CCl_4 \rightarrow CCl_2^+ + Cl_2 + e^-$$

although its negligible intensity prevented us from determining its appearance energy with accuracy; in the discussions of this section, we will therefore neglect it.

The study of the anion signal dependence on the target gas pressure shows that under our experimental conditions (60% attenuation of the positive ion beam), the two-collision mechanism is 24 times more probable than the one-collision mechanism. On average, there will thus be 1.96 collisions per affected CCl_2^+ projectile ion. Only two-step processes are relevant.

The $I^-/I^+(E_k)$ curve for $CCl_2^+ \rightarrow CCl_2^-$ upon collisions with Xe atoms, which is displayed in Fig. 8, shows a significant increase with a threshold located at 19.70 ± 1 eV. This corresponds to an excitation energy of $(19.7 - 15.3) = 4.4 \pm 1$ eV. As in the case of CCl^+, charge reversal is

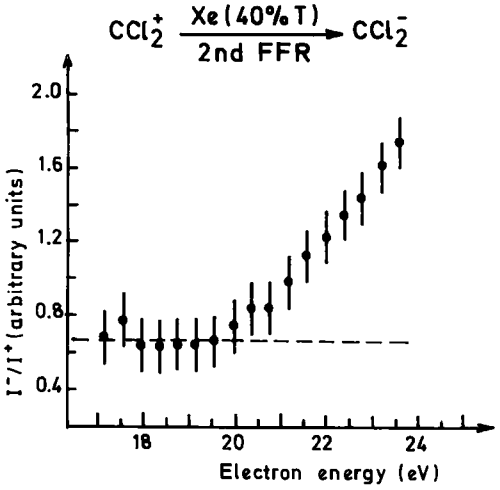

Fig. 8. Ratio of the anionic and cationic currents, I^-/I^+, for charge reversal of CCl_2^+ upon collision with Xe atoms. The transmittance of the positive ion beam is equal to 40%.

favoured at higher internal energies, which could also arise here from electronic excitation. The travel time to the collision cell, which is equal to 8.2 μs for CCl_2^+, gives an order of magnitude for the lifetime of this state.

Figure 9 shows the same curve when Kr is used to induce charge reversal. Here also, we observe an increase with a threshold at 19.5 $\pm$ 1 eV, corresponding to an excitation energy of 4.2 eV. Comparison of the data of Figs. 8 and 9 shows that the ratio of the charge reversal probability from the excited state to that from the ground state (P_1/P_0 with the notations of Section I.B) is 1.5 times larger with Kr than with Xe; in relative terms, the excited state plays a more important role when Kr is used.

In their previously cited work, Langford et al. [33] do not find any involvement of electronically excited states in the charge stripping of CCl_2^+. However, the relative intensities of the signals associated with the ground state and with an excited state in a given experiment depend on the cross-sections of the processes involved. The mechanisms of charge stripping and charge reversal are obviously very different: the fact that a given excited state is not observed in charge stripping does not necessarily preclude its observation in charge reversal, owing to a possibly larger cross-section in this latter case. There exists, to the best of our knowledge, no other information, either theoretical or experimental, on the long-lived electronic states of CCl_2^+, in particular the quartet states. To obtain complementary experimental information, we have studied the following metastable dissociation of CCl_2^+:

$$CCl_2^{+*} \rightarrow CCl^+ + Cl$$

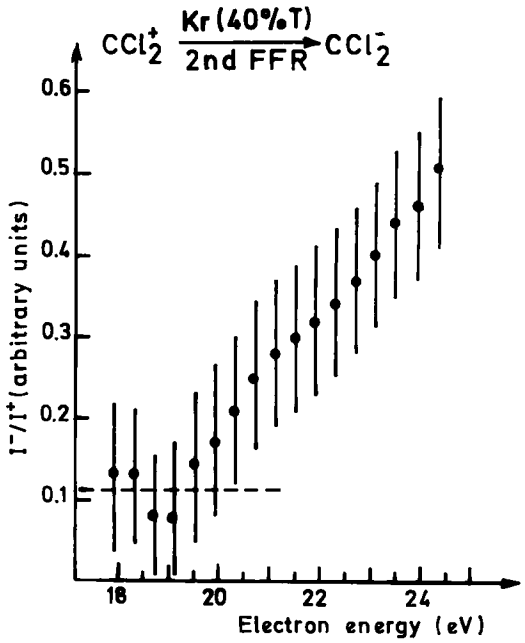

Fig. 9. Ratio of the anionic and cationic currents, I^-/I^+, for charge reversal of CCl_2^+ upon collision with Kr atoms. The transmittance of the positive ion beam is equal to 40%.

We have also performed semi-empirical MNDO calculations of the energies and equilibrium geometries of the ground and first excited states of this ion; the results of these studies are reported and discussed in the following paragraphs.

*B. The CCl_2^+ * → CCl^+ + Cl metastable dissociation*

Proctor et al. [14] have measured a value of 0.04 eV for the kinetic energy released on the fragments CCl^+ + Cl during the metastable dissociation of CCl_2^+. This suggests either the absence of any reverse activation barrier or that all the excess energy is converted into internal energy of CCl^+ and/or Cl.

We have measured the appearance energy for the CCl^+ fragment resulting from this metastable dissociation in both the first and the second field-free regions. The values obtained in both regions are in very good agreement: AE = 19.4 ± 0.4 eV. We have checked that the metastable signal remains strictly linear as a function of the CCl_4 ion source pressure, thus precluding the involvement of any collisionally-induced process. Our own determination of the kinetic energy release in the first field-free region leads to a value of 0.084 eV, in reasonable agreement with the value of Proctor et al. [14].

This value of the threshold energy for the metastable dissociation of CCl_2^+ is equal, within experimental error, to the energy where I^-/I^+ starts to increase in the charge reversal experiments (Figs. 8 and 9, Section III.A). If we consider, as we did in Section III.A., that the CCl_2^+ ions are produced by loss of two chlorine atoms from CCl_4^+, the measured appearance energy corresponds to an excitation energy of 4.1 eV. The threshold energy of 19.4 eV is 1.4 eV higher than the thermodynamical threshold for the following process:

$$CCl_4 \rightarrow CCl^+ + 3Cl + e^-$$

As only a small amount of this excess energy is released on the fragments, they must be produced with internal energy. The lowest excited state of Cl, $^2P_{1/2}$, has an energy of 0.11 eV with respect to the ground state, $^2P_{3/2}$. The energy of the next excited state is much too high (8.92 eV) to be taken into account. The first excited state of CCl^+ has an energy of 3.2 eV (see Section II.B) larger than the available excess energy. One is then left with the conclusion that CCl^+ is created at threshold with a large amount of vibrational energy.

It is therefore reasonable to consider that a long-lived excited state of CCl_2^+, lying 4.1 eV above the ground state, is responsible for both the metastable dissociation of this ion into the $CCl^+ + Cl$ channel and for the increase in the anion yield in charge reversal experiments. The lifetime of this state can be deduced to be larger than 8.2 μs, the time needed for CCl_2^+ ions to reach the second field-free region of our mass spectrometer. Since the measured excitation energy is larger than the lowest dissociation asymptote of CCl_2^+ (2.9 eV) [30], this excitation can only be of electronic nature. The next subsection is concerned with the elucidation of the nature of this excited state.

C. MNDO calculations of the first electronic states of CCl_2^+

The electronic configuration of the ground state of CCl_2 is

$$\ldots(2b_1)^2(2a_2)^2(7b_2)^2(9a_1)^2(3b_1)^0$$

Nguyen et al. [37] have calculated the energies of the first electronic states of CCl_2^+ obtained by removal of one electron from the valence orbitals. These calculations have been performed at the ab initio level with different basis sets, the largest one being 6-31G**; configuration interaction has been introduced using the Möller-Plesset perturbational method. All these calculations have been performed at the equilibrium geometry of the ground state $\tilde{X}^1A_1$ of CCl_2: r(C–Cl) = 1.736 Å; θ(ClCCl) = 110°; C_{2v} geometry. The calculated energies with respect to the neutral ground state CCl_2 $\tilde{X}^1A_1$ are summarized in the second column of Table 1. These vertical excitation energies cannot, however, be directly compared with the excitation energies which we deduce from appearance energy measurements, especially if the equilibrium geometries show strong variations from one state to the other.

TABLE 1

Energies and equilibrium geometries of the neutral and ionic states of CCl_2

State	Energy (eV)		Geometry	
	Ref. 37[a]	This work[b]	r(C–Cl) (Å)	θ(ClCCl) (°)
$CCl_2\tilde{X}^1A_1$	0.0	0.0	1.748	113.9
$CCl_2^-\tilde{X}^2B_1$		−2.24	1.843	110.1
$CCl_2^+\tilde{X}^2A_1$	9.75	9.83	1.586	160.5
$CCl_2^+\tilde{A}^2B_2$	11.85	12.62	1.778	82.8
$CCl_2^+\tilde{B}^2A_2$	12.29	13.22	1.766	113.0
$CCl_2^+\tilde{a}^4A_2$		13.20	1.662	134.2

[a] MP4SDQ/6-31G**; all the energies are calculated at the equilibrium geometry of the neutral ground state.

[b] For computational details, see text.

As far as the long-lived nature of the excited states is concerned, it can be argued that the $\tilde{A}^2B_2$ and $\tilde{B}^2A_2$ states become the two degenerate components of a $^2\Pi$ state for a linear Cl–C–Cl^+ geometry: these two states are therefore coupled by a Renner–Teller interaction. It is also very likely that the $\tilde{A}^2B_2$ and $\tilde{X}^2A_1$ states are coupled by a conical intersection involving the antisymmetrical valence vibration. It is therefore reasonable to expect that these doublet electronic states will have a lifetime shorter than 8×10^{-6} s (see Section III.B); conical intersections, for example, are known to bring about ultra-fast (10^{-14} s) intramolecular relaxation [38,39].

The quartet states, however, are expected to have a much longer lifetime because their relaxation to the ground state involves a spin-orbit interaction. We have therefore calculated the energies and equilibrium geometries of the first doublet and quartet states of CCl_2^+ at the MNDO level, using the AMPAC package [40]. Limited configuration interaction has been introduced: all the configurations resulting from excitations within the four external occupied orbitals and the LUMO have been taken into account. The equilibrium geometry of CCl_2 has been calculated to be r(C–Cl) = 1.748 Å; θ(ClCCl) = 113.9° (C_{2v} geometry), in good agreement with the ab initio values of Nguyen et al. [37]. The calculated energies for the neutral and ionic states are summarized in the third column of Table 1. These energies are adiabatic excitation energies; the corresponding equilibrium geometries are mentioned for each state. It can immediately be seen from these data that the first quartet state $\tilde{a}^4A_2$ (3.37 eV) has an energy which is compatible, within experimental error, with the experimental excitation energy deduced from Figs. 8 and 9 and from the appearance energy measured for the metastable dissociation $CCl_2^{+}* \rightarrow CCl^+ + Cl$. It is therefore reasonable to conclude that this state is responsible for the observed enhancement in the I^-/I^+ curve in the charge

reversal experiments. This state can also be the long-lived state involved in the above-mentioned metastable dissociation.

D. Discussion

Let us first of all consider in more detail the metastable process $CCl_2^+ * \rightarrow CCl^+ + Cl$. The following dissociation pathways are spin and symmetry allowed:

$$CCl_2^+(\tilde{a}^4A_2) \rightarrow CCl^+(a^3\Pi) + Cl(^2P_u)$$

$$CCl_2^+(\tilde{A}^2B_2) \rightarrow CCl^+(X^1\Sigma^+) + Cl(^2P_u)$$

$$CCl_2^+(\tilde{X}^2A_1) \rightarrow CCl^+(X^1\Sigma^+) + Cl(^2P_u)$$

However, the appearance energy of the metastable process considered here (19.4 eV) is lower than the energy required to produce $CCl^+ a^3\Pi$ fragments (21.04 eV). If we admit that the first quartet state $\tilde{a}^4A_2$ is the excited state involved, we have to explain how such a state can lead to CCl^+ fragments, which are, at least partly in their singlet ground state $X^1\Sigma^+$. This must involve a spin-orbit interaction leading to the relaxation of the quartet state into the doublet manifold, from which dissociation to the ground state CCl^+ fragment can occur. In order to gain an insight into the possible mechanisms of such relaxations, we have performed a cross-section in the potential energy surfaces of CCl_2^+ along the θ coordinate for a given r(C–Cl) internuclear distance (Fig. 10).

The analysis of the cross-sections displayed in Fig. 10 shows first of all that two $^2A_2$ states interact, leading to an avoided crossing around $\theta = 85°$. In this region, a mixing between the following configurations takes place:

$$\ldots(2b_1)^2(2a_2)^1(7b_2)^2(9a_1)^2(3b_1)^0 \quad {}^2A_2$$

$$\ldots(2b_1)^2(2a_2)^2(7b_2)^1(9a_1)^1(3b_1)^1 \quad {}^2A_2$$

A crossing between the $\tilde{a}^4A_2$ state, characterized by the following configuration

$$\ldots(2b_1)^2(2a_2)^2(7b_2)^1(9a_1)^1(3b_1)^1 \quad {}^4A_2$$

and the lowest energy $^2A_2$ state takes place for a value of the ClCCl angle equal to 92°, i.e. in the region of the non-adiabatic interaction between the two $^2A_2$ states. Since the spin-orbit operator is a monoelectronic operator, it will couple only configurations differing by at most one spin orbital: the above-mentioned triply excited configurations corresponding respectively to the doublet and the quartet multiplicity will therefore be coupled, leading to a non-radiative transition from $\tilde{a}^4A_2$ to $\tilde{B}^2A_2$. The magnitude of the spin-orbit

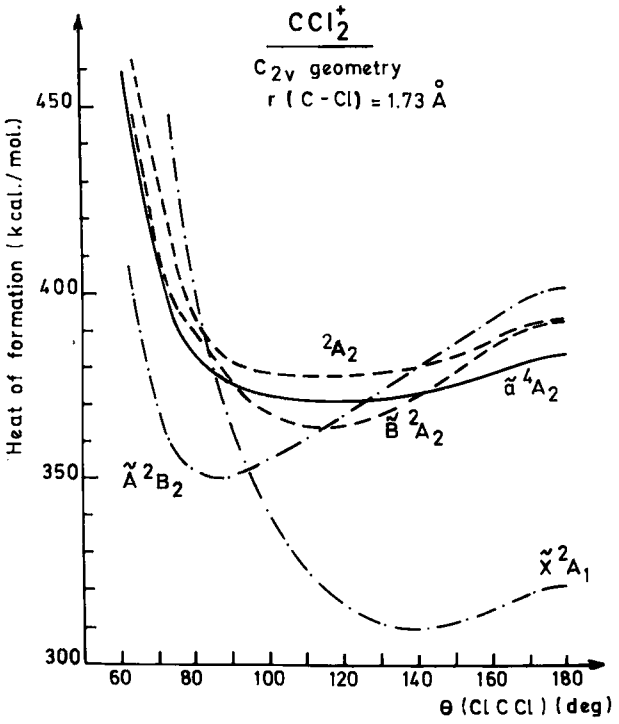

Fig. 10. Cross-section in the potential energy surfaces corresponding to the ground and first excited electronic states of CCl_2^+ as a function of the ClCCl angle. The C–Cl bond length is kept constant and equal to 1.73 Å. These calculations have been performed at the MNDO level with limited CI using the AMPAC package [40].

interaction increases rapidly with the nuclear charge: a medium-range value can be expected for CCl_2^+ which has two chlorine nuclei ($Z = 17$).

Once the $\tilde{B}^2A_2$ state has been reached, it can undergo a non-radiative transition to $\tilde{A}^2B_2$, via a Renner–Teller interaction. Unfortunately, the configuration interaction (CI) procedure of the AMPAC programme is not efficient enough to obtain an exact degeneracy of $\tilde{B}^2A_2$ and $\tilde{A}^2B_2$ at $\theta = 180°$, although the sizes of the corresponding CI submatrices are identical (10×10). Since the number of b_2 precursors in the core is higher than the number of a_2 precursors, the interelectronic repulsion is larger for the b_2 electrons; this asymmetry in the self-consistent field calculation can be only partially corrected in a limited CI procedure. The $\tilde{A}^2B_2$ state is in turn coupled with the ground ionic state via a conical intersection occurring for $\theta = 95°$. Such a coupling involves the antisymmetric valence vibration of B_2 symmetry. From this ionic ground state, dissociation leading to the ground state $CCl^+ + Cl$ fragments can take place.

This multi-step mechanism, which requires three internal conversions and involves both the symmetric and antisymmetric vibrational degrees of freedom, can be invoked to account for the metastability of the dissociation under study; the first step involves a spin-orbit interaction and thus leads to a decrease of the rate constant. Secondly, the complicated pathway the system must follow to reach the ground state is compatible with a significant vibrational excitation and thus with the small amount of kinetic energy released on the fragments.

Let us now go back to the charge reversal experiments. In Figs. 8 and 9, we observe an enhancement in the CCl_2^- yield at $E_k = 19.7\,eV$ when Xe or Kr are the target gases. As in the case of the CCl^+ charge reversal, we can observe that this effect seems to be governed by a resonance condition. The following processes are indeed resonant, within experimental error:

$$CCl_2^+(\tilde{a}^4A_2) + Xe(^1S) \rightarrow CCl_2(\tilde{X}^1A_1) + Xe^+(^2P_{1/2}) \quad (a)$$

$$CCl_2^+(\tilde{a}^4A_2) + Kr(^1S) \rightarrow CCl_2(\tilde{X}^1A_1) + Kr^+(^2P_{3/2}) \quad (b)$$

Starting from our experimental excitation energy for $\tilde{a}^4A_2$ (4.3 eV) and from the ionization energies of CCl_2 either from Lias et al. [30] or from Rademann et al. [36], we obtain a ΔH_r° value for reaction (a) of $-1.22\,eV$ according to ref. 30 and of $+0.04\,eV$ according to ref. 36. The corresponding ΔH_r° values for process (b) are $-0.66\,eV$ and $+0.60\,eV$. Despite the large discrepancy between the ionization energies derived by Lias et al. [30] and those of Rademann et al. [36], we see that, if we take into account our experimental uncertainty in the excitation energy, both processes can be considered as quasi-resonant. Once again, it should be pointed out that what really matters, strictly speaking, is the energy gap at the distance where charge exchange takes place. The calculation of potential energy hypersurfaces polarized by the approach of a rare gas is, however, exceedingly difficult. Our experimental results, both for CCl^+ and CCl_2^+, show that the resonance condition at infinite distance between the collision partners provides a good propensity rule for determining the most favourable charge exchange channel. These results concerning charge reversal are in agreement with a previous work of Keough et al. [41] who studied the charge reversal of Cl^+ with various target gases.

Other experimental studies on single-electron capture processes lead to the conclusion that the largest cross-sections are observed when the energy defect is small [42,43]. Such evidence for organic ions is shown, for example, in the work of Shields et al. [43] who measured by time-of-flight techniques the yield of fast neutrals resulting from Kiloelectronvolt neutralization of oxygen-containing organic ions and correlated this yield with the energy defect. This result is often used as an assumption allowing one to determine the internal energy contents of the fast neutrals resulting from neutralization. We wish, however, to point out that non-resonant processes are not necessarily negli-

gible as shown, e.g., by the present study (Figs. 3, 8 and 9) and by the recent data of Griffiths et al. [34]. Furthermore, in two-collision charge reversal experiments, the influence of the second step remains to be analysed in detail.

IV. CONCLUSION

Two major conclusions can be drawn from this study. Concerning CCl^+, we have confirmed by charge reversal experiments the long-lived nature (lifetime $> 6.2\,\mu s$) of the $a^3\Pi$ state, which had been observed in optical spectroscopy [32] and by high-resolution kinetic energy spectroscopy [33,34]. Concerning CCl_2^+, charge reversal experiments lead us to experimental evidence of a long-lived ($> 8.2\,\mu s$) electronic state: semi-empirical MNDO calculations allow us to assign this state to the first quartet state $\tilde{a}^4A_2$. We suggest that this state is also involved in the $CCl_2^{+*} \rightarrow CCl^+ + Cl$ metastable dissociation; according to the results of our MNDO calculations, we propose a multi-step relaxation sequence leading to the $CCl_2^+ \tilde{X}^2A_1$ ground state from which dissociation occurs. The first step of this sequence is a spin-orbit transition from the $\tilde{a}^4A_2$ state to the $\tilde{B}^2A_2$ state and leads to a significant decrease of the rate constant.

The second conclusion we would like to discuss is the involvement of these excited states in charge reversal experiments. Under our experimental conditions, charge reversal proceeds via two steps: neutralization of the cation, followed by anionization of this neutralized species. The second step will probably never be resonant, owing to the relatively small values of the electron affinities (0–5 eV). Our results on both CCl^+ and CCl_2^+ with the target gases Xe and Kr show that processes for which the first step is resonant (or quasi-resonant, owing to the experimental uncertainties in the excitation energy) are favoured. This result is in agreement with the conclusions drawn by Keough et al. [41]. In the cases studied here, the resonance condition is met upon excitation to a long-lived electronic state ($a^3\Pi$ for CCl^+, $\tilde{a}^4A_2$ for CCl_2^+). Since the number of excited state ions is certainly much smaller than the number of ground state ions, the relative cross-section must be much larger for the excited state under resonance conditions than for the ground state: otherwise a change in the I^-/I^+ curve would be scarcely detected. If this resonance condition is not met, we do not see any change in these curves: this is the case for charge reversal of CCl^+ with Kr, where we miss the $a^3\Pi$ state.

Our experimental observations are limited to the threshold region. Is this behaviour still the same at $E_k = 70$ eV, the energy at which most of the kinetic energy spectroscopy experiments are performed? It can be expected that, when E_k increases, the relative amount of ions which are in the ground state will increase due to internal conversions from excited states of the same multiplicity and that the effects observed in the present work will be of lesser

importance. It is therefore very difficult to compare collisional experiments of different types which are also performed at different E_k values; the fact that an excited state is not detected by charge stripping experiments at 70 eV [33], for example, does not preclude its observation in charge reversal experiments at threshold. The nature of the precursor must also be considered [34].

Other experiments would be interesting to obtain a deeper insight into these processes. We are now installing a differentially-pumped collision cell in the first field-free region in order to have a second time window at shorter times. We wish to check if the CCl^+ $A^1\Pi$ state, which has a lifetime of 3.9 μs [31], is also involved in charge reversal. This will also allow us to study in more detail the dissociation mechanisms of the anions produced by charge reversal. This will be discussed in a forthcoming paper.

ACKNOWLEDGEMENTS

We are indebted to Professors J.C. Lorquet, J. Collin and J. Momigny for a critical reading of the manuscript and for stimulating suggestions. We are grateful to Pierre Mélon for his invaluable assistance. The financial contributions of the Fonds National de la Recherche Scientifique (Belgium), of the Fonds de la Recherche Fondamentale Collective (Belgium), of the Communauté Française de Belgique (Action de Recherches Concertées) and of the University of Liège are gratefully acknowledged.

REFERENCES

1 F.W. McLafferty (Ed.), Tandem Mass Spectrometry, Wiley-Interscience, New York, 1983.
2 K.L. Busch, G.L. Glish and S.A. McLuckey, Mass Spectrometry/Mass Spectrometry, VCH, Weinheim, 1988.
3 F.W. McLafferty, P.F. Bente III, R. Kornfield, S.C. Tsai and I. Howe, J. Am. Chem. Soc., 95 (1973) 2120.
4 F.W. McLafferty, R. Kornfeld, W.F. Haddon, K. Levsen, I. Sakai, P.F. Bente III, S.C. Tsai and H.D.R. Schuddemage, J. Am. Chem. Soc., 95 (1973) 3886.
5 R.G. Cooks (Ed.), Collision Spectroscopy, Plenum Press, London, 1978.
6 P.J. Todd and F.W. McLafferty, Int. J. Mass Spectrom. Ion. Phys., 38 (1981) 371.
7 C. Wesdemiotis and F.W. McLafferty, Chem. Rev., 87 (1987) 485.
8 J.K. Terlouw and H. Schwarz, Angew. Chem., 99 (1987) 829.
9 J.L. Holmes, Mass Spectrom. Rev., 8 (1989) 513.
10 F.W. McLafferty, Science, 247 (1990) 925.
11 J.H. Beynon, Anal. Chem., 42 (1970) 97A.
12 R.G. Cooks, J.H. Beynon and T. Ast, J. Am. Chem. Soc., 94 (1972) 1004.
13 T. Ast, J.H. Beynon and R.G. Cooks, J. Am. Chem. Soc., 94 (1972) 6611.
14 C.J. Proctor, C.J. Porter, T. Ast and J.H. Beynon, Int. J. Mass Spectrom. Ion Phys., 41 (1982) 251.
15 R.G. Cooks, T. Ast, B. Kralj, V. Kramer and D. Zigon, J. Am. Soc. Mass Spectrom., 1 (1990) 16.

16 J.H. Bowie and T. Blumenthal, J. Am. Chem. Soc., 97 (1975) 2959.
17 G.A. McClusky, R.W. Kondrat and R.G. Cooks, J. Am. Chem. Soc., 100 (1978) 6045.
18 T. Keough, J.H. Beynon and R.G. Cooks, J. Am. Chem. Soc., 95 (1973) 1695.
19 T. Keough, J.H. Beynon and R.G. Cooks, Chem. Phys., 12 (1976) 191.
20 R. Feng, C. Wesdemiotis and F.W. McLafferty, J. Am. Chem. Soc., 109 (1987) 6521.
21 S. Villeneuve and P.C. Burgers, Org. Mass Spectrom., 21 (1986) 733.
22 R.S. Mercer and A.G. Harrison, Org. Mass Spectrom., 22 (1987) 710.
23 F.M. Harris and B.C. Cooper, Int. J. Mass Spectrom. Ion Processes, 97 (1990) 165.
24 H. Wankenne and J. Momigny, Int. J. Mass Spectrom. Ion Phys., 7 (1971) 227.
25 J.H. Beynon, R.G. Cooks, K.R. Jennings and A.J. Ferrer-Correia, Int. J. Mass Spectrom. Ion Phys., 18 (1975) 87.
26 G.H. Wannier, Phys. Rev., 90 (1953) 817.
27 W.J. Griffiths and F.M. Harris, Int. J. Mass Spectrom. Ion Processes, 85 (1988) 69.
28 H.M. Rosenstock, K. Draxl, B.W. Steiner and J.T. Herron, J. Phys. Chem. Ref. Data, 6 (suppl. 1) (1977).
29 G. Tornow, R. Locht, R. Kaufel and H. Baumgärtel, Int. J. Mass Spectrom. Ion Processes, submitted.
30 S.G. Lias, J.E. Bartmess, J.F. Liebman, J.L. Holmes, R.D. Levin and W.G. Mallard, J. Phys. Chem. Ref. Data, 17 (suppl. 1) (1988).
31 H.A. Van Sprang, H.H. Brongersma and F.J. De Heer, Chem. Phys., 35 (1978) 51.
32 M. Tsuji, T. Mizuguchi, K. Shinohara and Y. Nishimura, Can. J. Phys., 61 (1983) 838.
33 M.L. Langford, M. Hamdan and F.M. Harris, Int. J. Mass Spectrom. Ion. Processes, 95 (1990) 243.
34 W.J. Griffiths, F.M. Harris and J.D. Barton, Rapid. Commun. Mass Spectrom., 3 (1989) 384.
35 J.C. Lorquet, B. Leyh-Nihant and F.W. McLafferty, Int. J. Mass Spectrom. Ion Processes, 100 (1990) 465.
36 K. Rademann, H.W. Jochims and H. Baumgärtel, J. Phys. Chem., 89 (1985) 3459.
37 M.T. Nguyen, M.C. Kerins, A.F. Hegarty and N.J. Fitzpatrick, Chem. Phys. Lett., 117 (1985) 295.
38 M. Desouter-Lecomte, D. Dehareng, B. Leyh-Nihant, M.-Th. Praet, A.J. Lorquet and J.C. Lorquet, J. Phys. Chem., 89 (1985) 214.
39 H. Köppel, W. Domcke and L.S. Cederbaum, Adv. Chem. Phys., 57 (1984) 59.
40 The AMPAC package, containing the MINDO/3, MNDO and AM1 methods, has been written by the Dewar Research Group, Chemistry Department, The University of Texas, Austin, TX 78712. It has been converted for an IBM 3090 computer by R. Farren and E.R. Davidson, Department of Chemistry, Indiana University, Bloomington, IN 47405. It is distributed by Quantum Chemistry Program Exchange under reference number 539.
41 T. Keough, J.H. Beynon and R.G. Cooks, Int. J. Mass Spectrom. Ion Phys., 16 (1975) 417.
42 G. Gellene and R.F. Porter, Acc. Chem. Res., 16 (1983) 200.
43 G.C. Shields, P.A. Steiner IV, P.R. Nelson, M.C. Trauner and T.F. Moran, Org. Mass Spectrom., 22 (1987) 64.